International Journal of Science and Research Archive

eISSN: 2582-8185

Cross Ref DOI: 10.30574/ijsra

Journal homepage: https://ijsra.net/

(RESEARCH ARTICLE)

Check for updates

The biosynthesis of nickel oxide nanoparticles using watermelon rind extract and their biophysical effects on the germination of *Vigna radiata* seeds at various concentrations

Mohd Kashif Aziz [1,*], Sudhakar Chauhan [1], Zeba Azim [2], Gyanendra Kumar Bharati [1] and Shekhar Srivastava [1]

[1] *Department of Chemistry, University of Allahabad, Prayagraj, U.P., India -211002.*
[2] *Plant Physiology Laboratory, Department of Botony, University of Allahabad, Prayagraj, U.P., India - 211002.*

International Journal of Science and Research Archive, 2022, 07(02), 245–254

Publication history: Received on 15 October 2022; revised on 24 November 2022; accepted on 26 November 2022

Article DOI: https://doi.org/10.30574/ijsra.2022.7.2.0271

Abstract

Unique and bio-inspired synthesis of nickel oxide nanoparticles by using an innocuous and ecofriendly waste material that is watermelon rind. In the reaction, watermelon rind recycled and used its extract as a solvent which act as a reductant for a synthesis of nickel oxide nanoparticle. The synthesized NiO NPs were analyzed by using X-ray Diffraction (XRD), transmission electron microscopy (TEM), Fourier transform infrared spectroscopy (FTIR) and UV-Vis spectroscopy. FTIR peak at 745 cm-1 and 671 cm-1 indicated that the formation of Ni-O bond. A prominent peak of UV-Vis spectra at 283 nm and band gap, calculated with the help of UV data, was ~3.3 eV. The obtained PXRD pattern and JCPDS data suggested the formation of nickel oxide nanoparticle and the average crystallite size calculated by Scherrer's equation in between 30 to 150 nm. The average grain size of NiO NPs perceived from TEM images was 46.55 nm and polygonal barrel shape particles. Since, a simple, straightforward, pollutant-free, and economical technique for the synthesis of nickel oxide nanoparticles. However, the above synthesized nickel oxide nanoparticles have been explored for biophysical parameter vis. radicle length, plumule length and germination percentage on a *Vigna radiata* (moong) seed by the treatment of some concentration i.e. 25 ppm, 50 ppm, 100 ppm and 200 ppm in germination processes. At a low concentration of 25 ppm, a beneficial improvement in the germination process of *Vigna radiata* seed was observed.

Keywords: Watermelon rind extract (WRE); Biophysical activity; FTIR; XRD and germination

1. Introduction

In the past two decades, nano synthesis of various compounds became an interest to the researcher. Various nanostructured material shows a unique chemical and physical properties which explore the application in the core subjects of physics, chemistry, biology,etc like morphology, size, shape, antimicrobial activities, germination, crystallography and many more (1–3). Nickel is an important transition metal which have extensive properties with their oxides of nanoparticles because of their physiochemical properties like surface, electrical, optical and magnetic activities (4,5). Nickel oxide nanoparticle has p-type semiconductor with a high optical energy band gap due to the oxygen occupancy in the lattice structure (6,7). Nickel oxide nanoparticles shows a cubic lattice structure with a widespread applications such as photoelectron devices, catalysis, gas sensors, thermoelectric materials, fuel cells, anticancer, cytotoxicity, nonenzymatic glucose sensors, germination, dye-sensitized photocathodes, etc. (8–10). Green synthesis of nanoparticles is perform by several approaches such as chemical vapor deposition (11), microemulsion (12), coprecipitation (11), hydrothermal (13), pulsed laser ablation (14) and sol-gel (15,16). Above all other approaches, sol-gel method is best for the green synthesis because it is simple, easy to handle, not much harmful to the ecosystem;

* Corresponding author: Mohd Kashif Aziz
Department of Chemistry, University of Allahabad, Prayagraj, U.P., India -211002.

cost effective and production of high purity due to the main composition of extract directly involved in the reaction (17). In the study of literatures, we found that many of the metal oxides nanoparticles synthesized via green synthetic approaches; many of them uses a waste material of fruit which are discarded in a garbage of municipal in India. Hence, in this paper, we used a naturally available plentiful waste i.e. watermelon rinds extract of fresh watermelon to synthesize nickel oxide nanoparticles via green synthetic approaches.

Watermelon is naturally abundant climbing plant of *Cucurbitaceae* family called *Citrullus lanatus*. It is advantageous warm seasonal fruit which is widely available at tropical and subtropical region. Watermelon is a large fleshy fruit which is poised with flesh (edible part), seed (thoroughly dispersed in flesh) and rind (waste part of the fruit which contribute approximately 35% of the total weight) (18,19). The watermelon rind (WR) ordinarily discarded and had no commercial value but many people of tribal areas used as a vegetable (20). In the literature survey of watermelon rind we found that they contain an antioxidants due to richness of hydroxyl and carboxyl functional groups (20). Watermelon rind consist of copious of fibre, citrulline, vitamin and minerals; it has also a higher moisture, proteins, pectin, carbohydrate, carotenoids, ash content and 17 % crude fibre which is very high (21).

In the literature, we found that several plants has been used to prepare a nickel oxide nanoparticles which have antiviral, antifungal, antibacterial activities, etc.(22–29) and severals metal oxide NPs were used in germination processes of many seeds like tomato, oil seed rape, pumkin, etc. (30–33). Nickel oxide is a promising P-type semiconductor, due to a non-stoichiometric structural flaw and its high activity in the breakdown of phenol and its derivatives (34,35). Watermelon rind extract is suitably used as a reducing agent in a world of green synthetic chemistry to the present experimental work because they are rich in phenolic components.

In this research paper, the experimental works are carried out by Watermelon Rind Extract which is suitable for the synthesis of Nickel Oxide nanoparticles just because of phenolic, hydroxyl and carboxyl component availability in Watermelon Rind Extract and they act as a reductant in the process (36). The synthesized Nickel Oxide NPs were characterized by X-Ray Diffraction, UV-visible spectroscopy, Infrared spectroscopy and Transmission Electron Microscopy. The green synthesized nickel oxide nanoparticles are applied on a *Vigna radiata* (cow pea) to see the effect in a process of germination.

2. Experimental Method

In synthesis of Nickel oxide nanoparticles, we are collecting a watermelon rind and washed several times by double distilled water; then it is thoroughly grind in a mixer grinder. Filtering all the extract through a sterile steel sieve and after that it will filter through a cotton fittig in a conical funnel to remove extra residue of watermelon rind. Finally, we took 50 ml of pure watermelon rind extract (WRE) as a solvent in a burette by filtering through a whatman filter paper grade 1.

$NiCl_2.6H_2O$ (Nickel chloride hexahydrate) salt used as a precursor in the reaction involved for the preparation of NiO NPs. The above nickel salt is of analytical grade and used as without additional purification.

In a round bottam flask, 20 ml of 0.1 M of $NiCl_2.6H_2O$ and 50 ml of watermelon rind extract (WRE) in a burette. Aqueous solution of 20 ml of 0.1 M $NiCl_2.6H_2O$ is placed on magnetic stirrer and WRE added dropwise with a rate of 1 drop per second with continuous stirring at a speed of 300 rotation per minute. After adding all the 50 ml of WRE, we raise a temperature from 25°C to 80°C and fix the spiral reflux condenser with a continuous stirring for 12 hours until turbidity was seen in reaction mixture. Thus, the sticky gel was formed which was green in color and discard the supernatant liquid after settling and washed through a double distilled water. Then, the sample was allowed to dry in an oven at 70°C for 10 hours and the dried powder was grind in an agate mortar pestle. Finally, the sample was put in a heating mantle in an open air at approximate temperature of 200°C for 10 hours and again grind through agate mortar pestle. The black color NiO NPs sample was prepared for further analysis

The FTIR (Fourier Transform Infrared spectroscopy) of NiO NPs were recorded by Bruker Alpha Instrument via attenuated total reflection (ATR) mode spectrophotometer of range 4000 – 500 cm^{-1} wavenumber with a resolution of 2 cm^{-1} at Standard Temperature and Pressure (STP). The powdered X-Ray Diffraction was analysed by a Philips X'pert Model XRD in the range of $2\theta = 10 – 80$ degree by using a Cu-Kα X-rays of wavelength $\lambda = 1.54$ Å. The UV-Visible spectra of a sample were investigated by ELICO SL-210 double beam spectrophotometer instrument with a wave length range of 190 – 900 nm and the Transmission Electron Microscopy (TEM) imaging technique were used in a sample by FEI-Tecnai-Netherland of model G2F30S-Twin with an accelerating voltage of 300 kV.

The preparation of germination process was firstly occurred by the purchasing a good quality seed of *Vigna radiata* from registered seed merchant for an experiments. The experimental seed were properly clean and soaked for 7 hours with proper aeration at STP. Nickel oxide nanoparticles were prepared in four different concentration in a double distilled water for a treatment in germination process of *Vigna radiata* seeed i.e. T_1 = 25 ppm, T_2 = 50 ppm, T_3 = 100 ppm and T_4 =200 ppm; for proper particle distribution applying ultrasonicator for 20 minutes in all the concentration (T_1-T_4). One set of seed taken as control that is only in double distilled water called as control (C). The seeds of *Vigna radiata* took in a pair and soaked with 30 ml of different concentrations from T_1 to T_4 for 5 hours. After the treatment of *Vigna radiata* seeds, they are transferred in a petriplate lined with Whatman No.1 filter papers and put in a dark place for a germination process for 6 days and every alternate day seedling length of germination were recorded.

3. Results and Discussion

3.1. X-Ray Diffraction Analysis

This one is the preliminary investigative technique for the confirmation of nanoparticle synthesis for a further analysis. The average grain size of nickel oxide nanoparticle were determined by the Debye-Scherrer formulae (37).

$$D = 0.9\lambda / (\beta \cos\theta)$$

Where,

D = Particle size of the sample
λ = X-ray wavelength
β = FWHM (full width half-maxima) of a peak in a radian
θ = angle of diffraction called Bragg angle

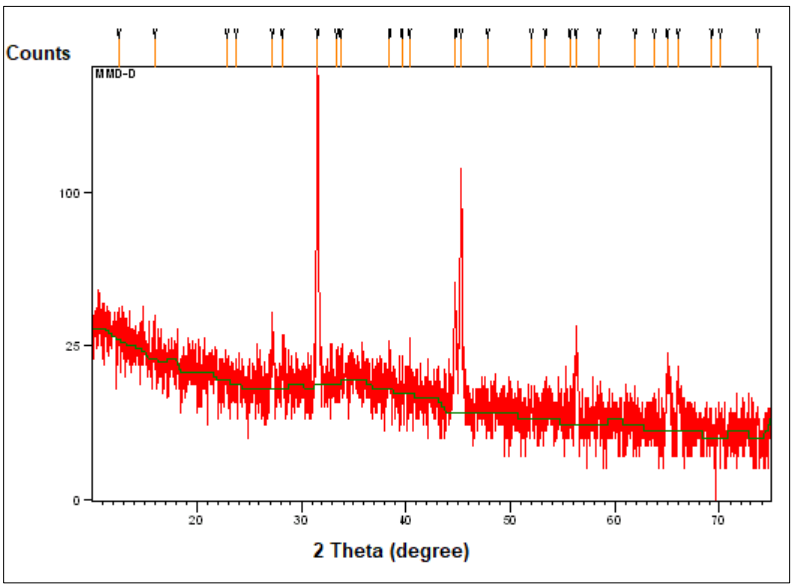

Figure 1 XRD image of Nickel Oxide NPs synthesized by using WRE

In figure 1, the XRD peaks of the synthesized sample revealed that the formation of cubic phase nickel oxide (NiO) nanoparticle crystals at an angle 2θ of 37.6359, 43.2487, 62.9821 and 74.9835 (JCPDS Card 78-0423) alongwith the other peaks of Ni_2O_3 at an angle 2θ of 31.5129, 56.2633 and 66.0285 (JCPDS Card 14-0481). In the Fig.1, the extra peaks and noises is due to the extra residues of the WRE which show the interruption in the XRD analysis peaks but this was just because we don't put in a high temperature calcination, in which further application we have to conduct in a germination process. The crystallite size of a NiO NPs are in a range of 30 nm to 150 nm from the above XRD data by calculating the debye-scherrer formula shown in a Table 1.

Table 1 Debye-scherrer formula

Angle (2θ) experimental	FWHM	d-value (Å) experimental	d-value (Å) standard	Identification (XRD Standard data)	Crystallite Size (nm)
37.6359	0.2362	2.4097	2.4127	NiO [111]	37.13
43.2487	0.0984	2.0761	2.0895	NiO [200]	90.75
62.9821	0.0787	1.4814	1.4775	NiO [220]	123.70
74.9835	0.1920	1.2638	1.2600	NiO [311]	54.50
31.5129	0.1378	2.8390	2.8424	Ni_2O_3 [002]	62.59
56.2633	0.1968	1.6350	1.6383	Ni_2O_3 [202]	47.83
66.0285	0.3149	1.4150	1.4190	Ni_2O_3 [004]	31.44

3.2. Fourier Transform Infrared Spectral Analysis

The identification of functional group and other stretching between all the bonds are analyzed by fourier transform infrared spectrum within the range of 400 cm^{-1} to 4000 cm^{-1}. In figure 2, the FTIR spectra of NiO NPs synthesized by using green synthetic approach by WRE as a reductant to identify the nature of molecular bond present in it.

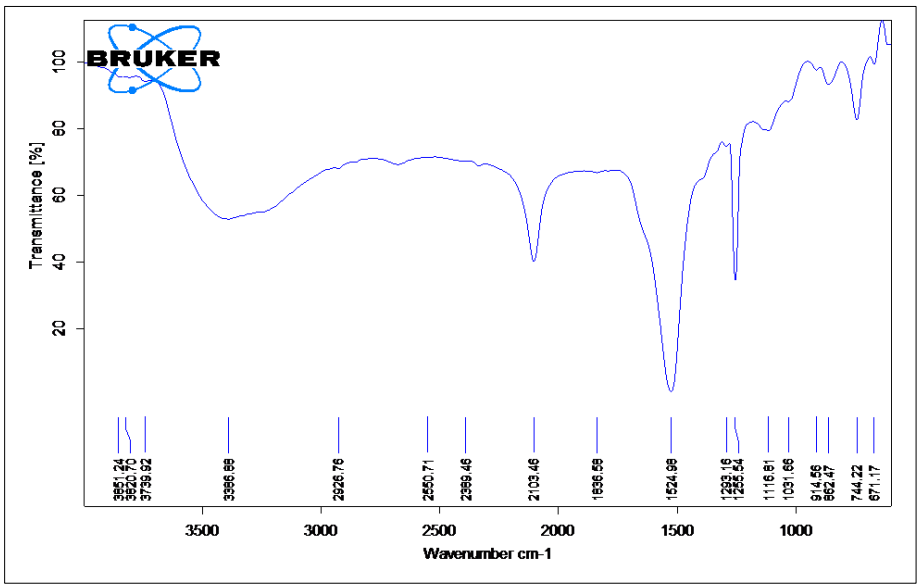

Figure 2 FTIR data of NiO – NPs synthesized via WRE

A characteristic wide and intense band centered peak of $Ni(OH)_2$ due to –OH stretching vibration and interlayer water molecules interference at 3368 cm^{-1}. The intense peak at 1524 cm^{-1} is due to the bending of H_2O molecule. At 1260 cm^{-1} peak band were observed due to the symmetric and asymmetric stretching vibrations of CO_2 molecule. Vibrational peaks of NiO NPs were observed in between 400 cm^{-1} to 850 cm^{-1}(38). The bunsenite phase of NiO is observed at peak 671 cm^{-1} (39), although another strong peak at 745 cm^{-1} of Ni – O bond vibration (38).

3.3. UV-VIS Spectroscopy Analysis

The UV-Vis examination was detected under a wavelength of 200 – 500 nm. Figure 3A graph represents the UV – Vis spectra of NiO NPs was achieved by ultrasonicator dispersion method in double distilled water. A prominent absorption peak is witnessed at a wavelength of 283 nm. The absorption of nanoparticles in an UV area is endorsed to energy band gap absorption (40).

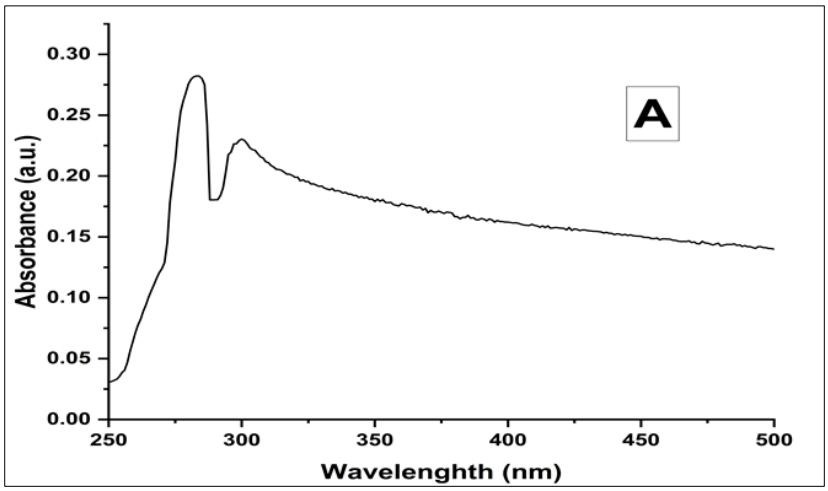

Figure 3A UV-Vis spectra of Nickel oxide nanoparticle by ELICO SL-210 UV-Vis spectrophotometer

The energy band gap was determined by using Tauc relation (41).

$$\alpha h\nu = \alpha\,(h\nu - E_g)^n \ldots\ldots\ldots\ldots \textit{Tauc Equation.}$$

Where,

α = Absortption coeficient
$h\nu$ = Photon energy
E_g = Energy band gap
n = ½ - direct band gap transition; 2 – indirect band gap transition.

Hence, the energy band gap for an absorption peak can be achieved by extrapolating the exponential portion of the curve (Ahυ) n–hυ to the starting point. Figure 3B shows the $(\alpha h\nu)^2$ versus hν graph for a NiO NPs sample for obtaining an energy band gap.

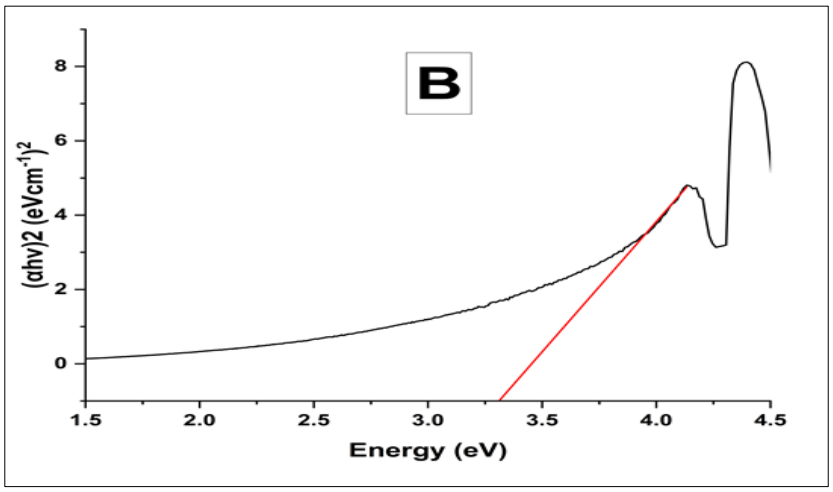

Figure 3B Energy band gap of nickel oxide NPs by calculating the UV-vis data through tauc equation

The energy band gap of NiO NPs is 3.3 eV, which is lesser than bulk (42). The energy band gap is directly correlated with the grain size of a nanoparticle, and higher the annealing temperature can be used to minimize any chemical defects or vacancies that may be present in a sample crystal. This process also produces slight shifts in shorter wavelengths, which can go through direct transition (n=1/2) to lower band gap energies (40,43,44). The energy band gap of semiconductor nanoparticles also increases with decreasing grain size, as is well known. They do not experience the quantum confinement effect because of their smaller Bohr radii.

3.4. Transmission Electron Microscopy (TEM)

The Transmission Electron microscopy (TEM) analysis can reveal the morphology and size of NiO NPs in their study. In Figure 4 (A, B and C), the TEM images of NiO NPs shows that their morphology is polyhedral crystal sphere which look like a barrel shape and the average particle size is 46.55 nm. This is very precise experimental data related to XRD which shows the size calculated by using Scherrer's formulae.

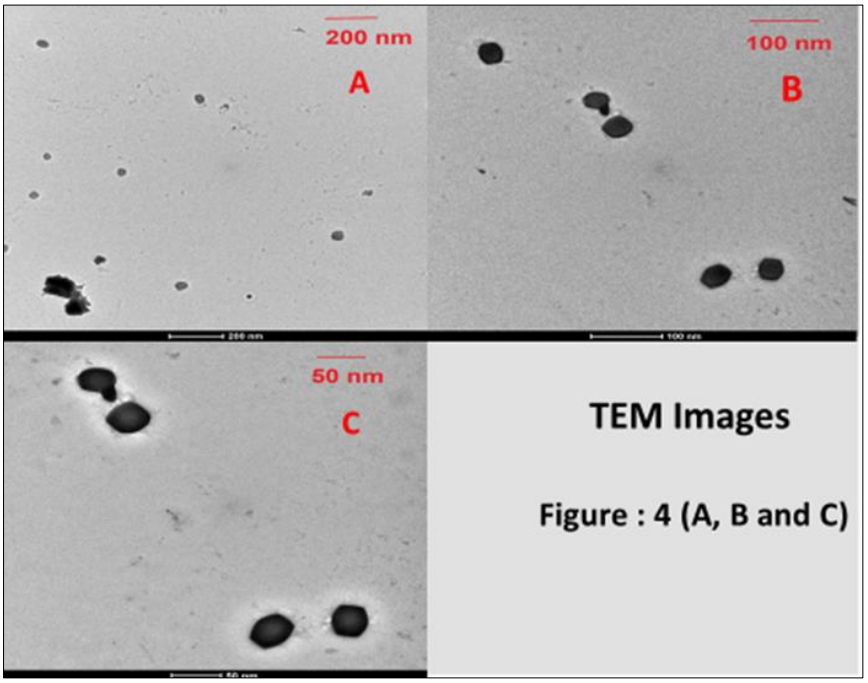

Figure 4 TEM images of Nickel oxide NPs; A, B and C showing a comparative magnification i.e. 200 nm, 100 nm and 50 nm, respectively

3.5. Investigation of germination in Vigna radiata seed

In a petriplate assay, after a treatment of NiO nanoparticles in parts per million it affects all the biophysical parameters; some of them analyzed in a treatment are radicle length, plumule length and germination percentage. After a 6th day of treatments with a dissimilar concentration of NiO NPs (T_1-T_4) in a *Vigna radiata* seed, the figure 5 illustrate the process of a biophysical activity via graph of the radicle length, plumule length and germination percentage. The *Vigna radiata* seed which is treated with a lower concentration i.e. 25 ppm (T_1) shows a significant growth in germination processes. All the treatments along with a control experiment were recorded in a pair of seed after the 6th day of germination processes which shown in a figure 6. The significant augmentation was recorded in a seed was demonstrate by a graph in a figure 5 which shows a germination percentage, plumule length and radicle length by 18 %, 12 % and 10 % respectively over control treatment. As seeds undergo sprouting, nanoparticles have a propensity to enter the seed coats, causing an increase in growth (45). At lower concentration many of the nanoparticles are advantageous for growth (Ce – NPs), metabolism (CeO – NPs) and biophysical & biochemical activity (ZnO – NPs) (46,47).

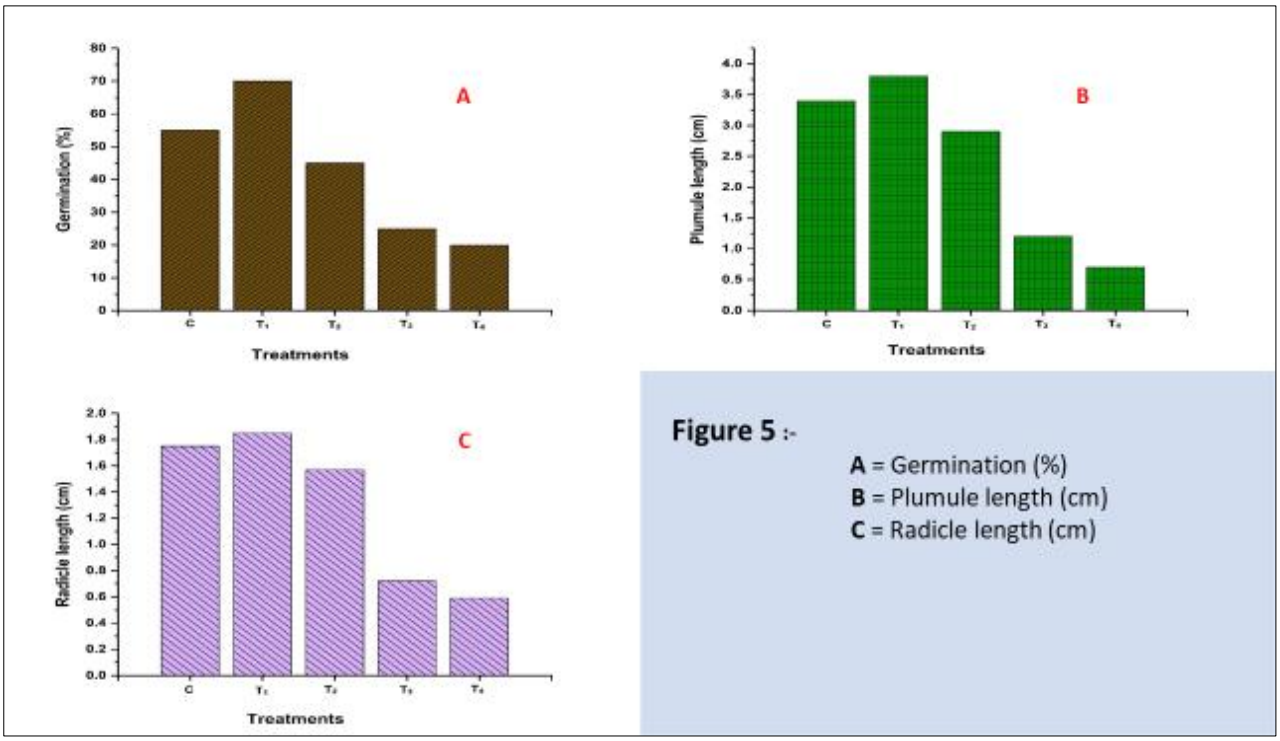

Figure 5 Graphically demonstrate the biophysical activity in germination process of *Vigna radiata* seed

Figure 6 Original Image click by smartphone along with measuring scale of *Vigna radiata* seed after the 6th day of germination

4. Conclusion

Using watermelon rind extract, we have demonstrated a unique green synthesis of nickel oxide nanoparticles. FTIR and XRD data established that the assembly of nickel oxide nanoparticles in an experiment with cubic structure along with space group Fm3/m. The optical properties of a produced nanoparticles exhibit a remarkable UV-Vis spectrometer absorbance at 283 nm wavelength and band gap energy is 3.3 eV, which show a very effective for further applications. TEM analysis show the barrel shape images of nickel oxide nanoparticle which have an average particle size of 46.55 nm. Experimental testing was done on the synthesized nickel oxide nanoparticle to assess its bioactivities on the germination of Vigna radiata seeds and seen the positive reactions at smaller concentrations in compared to a controlled experiment, but nanoparticles at high concentrations were observed to be detrimental to germination processes.

Overall, the suggested green synthetic approach is easy to apply and environmentally beneficial because it doesn't call for any additional reductants and the efficacy of the aforementioned technique for producing a brilliant catalysts for usage in a broad series of organic reactions. Thus, we can draw the conclusion that NiO NPs tend to have a favorable response up to a specific concentration but that as concentration increases, they have an adverse effect on the biological system.

Compliance with ethical standards

Acknowledgments

The author acknowledges the Professor N. B. Singh in Botany Department, University of Allahabad, for providing the facility for seedling processes. Also, the authors are thankful to IIT, Bombay and Central University of Punjab, for providing the analysis through the SAIF facility.

Disclosure of conflict of interest

There is no conflict of interest was reported by authors.

References

[1] Kalam A, Al-Sehemi AG, Al-Shihri AS, Du G, Ahmad T. Synthesis and characterization of NiO nanoparticles by thermal decomposition of nickel linoleate and their optical properties. Mater Charact [Internet]. 2012;68:77–81. Available from: http://dx.doi.org/10.1016/j.matchar.2012.03.011

[2] Al-Sehemi AG, Al-Shihri AS, Kalam A, Dud G, Ahmad T. Microwave synthesis, optical properties and surface area studies of NiO nanoparticles. J Mol Struct [Internet]. 2014;1058(1):56–61. Available from: http://dx.doi.org/10.1016/j.molstruc.2013.10.065

[3] Singh J, Dutta T, Kim KH, Rawat M, Samddar P, Kumar P. "Green" synthesis of metals and their oxide nanoparticles: Applications for environmental remediation. J Nanobiotechnology [Internet]. 2018;16(1):1–25. Available from: https://doi.org/10.1186/s12951-018-0408-4

[4] Gleiter H. Nanocrystalline materials. Prog Mater Sci. 1989;33(4):223–315.

[5] Schmid G. Nanoparticles ¨ nter Schmid Edited by Gu. Nanotechnology. 2004. 1–434 p.

[6] Chen HL, Lu YM, Hwang WS. Characterization of sputtered NiO thin films. Surf Coatings Technol. 2005;198(1-3 SPEC. ISS.):138–42.

[7] Yang H, Tao Q, Zhang X, Tang A, Ouyang J. Solid-state synthesis and electrochemical property of SnO2/NiO nanomaterials. J Alloys Compd. 2008;459(1–2):98–102.

[8] Ezhilarasi AA, Vijaya JJ, Kennedy LJ, Kaviyarasu K. Green mediated NiO nano-rods using Phoenix dactylifera (Dates) extract for biomedical and environmental applications. Mater Chem Phys [Internet]. 2020;241(November 2019):122419. Available from: https://doi.org/10.1016/j.matchemphys.2019.122419

[9] Fardood ST, Ramazani A, Moradi S. A novel green synthesis of nickel oxide nanoparticles using arabic gum. Chem J Mold. 2017;12(1):115–8.

[10] Sabouri Z, Akbari A, Hosseini HA, Khatami M, Darroudi M. Green-based bio-synthesis of nickel oxide nanoparticles in Arabic gum and examination of their cytotoxicity, photocatalytic and antibacterial effects. Green Chem Lett Rev [Internet]. 2021;14(2):402–12. Available from: https://doi.org/10.1080/17518253.2021.1923824

[11] Rahman MA, Radhakrishnan R, Gopalakrishnan R. Structural, optical, magnetic and antibacterial properties of Nd doped NiO nanoparticles prepared by co-precipitation method. J Alloys Compd [Internet]. 2018;742:421–9. Available from: https://doi.org/10.1016/j.jallcom.2018.01.298

[12] Du Y, Wang W, Li X, Zhao J, Ma J, Liu Y, et al. Preparation of NiO nanoparticles in microemulsion and its gas sensing performance. Mater Lett. 2012;68:168–70.

[13] Ma J, Lian J, Duan X, Liu X, Zheng W. α-Fe2O3: Hydrothermal synthesis, magnetic and electrochemical properties. J Phys Chem C. 2010;114(24):10671–6.

[14] Rane AV, Kanny K, Abitha VK, Thomas S, Thomas S. Methods for Synthesis of Nanoparticles and Fabrication of Nanocomposites [Internet]. Synthesis of Inorganic Nanomaterials: Advances and Key Technologies. Elsevier Ltd.; 2018. 121–139 p. Available from: http://dx.doi.org/10.1016/B978-0-08-101975-7.00005-1

[15] Turgut G, Sonmez E, Duman S. Determination of certain sol-gel growth parameters of nickel oxide films. Ceram Int [Internet]. 2015;41(2):2976–89. Available from: http://dx.doi.org/10.1016/j.ceramint.2014.10.133

[16] Fakhari S, Jamzad M, Kabiri Fard H. Green synthesis of zinc oxide nanoparticles: a comparison. Green Chem Lett Rev. 2019;12(1):19–24.

[17] Darroudi M, Sabouri Z, Kazemi Oskuee R, Khorsand Zak A, Kargar H, Hamid MHNA. Sol-gel synthesis, characterization, and neurotoxicity effect of zinc oxide nanoparticles using gum tragacanth. Ceram Int [Internet]. 2013;39(8):9195–9. Available from: http://dx.doi.org/10.1016/j.ceramint.2013.05.021

[18] Pérez J, Gómez K, Vega L. Optimization and Preliminary Physicochemical Characterization of Pectin Extraction from Watermelon Rind (Citrullus lanatus) with Citric Acid. Int J Food Sci. 2022;2022.

[19] Rico X, Gullón B, Alonso JL, Yáñez R. Recovery of high value-added compounds from pineapple, melon, watermelon and pumpkin processing by-products: An overview. Food Res Int [Internet]. 2020;132(December 2019):109086. Available from: https://doi.org/10.1016/j.foodres.2020.109086

[20] Al-Sayed HMA, Ahmed AR. Utilization of watermelon rinds and sharlyn melon peels as a natural source of dietary fiber and antioxidants in cake. Ann Agric Sci [Internet]. 2013;58(1):83–95. Available from: http://dx.doi.org/10.1016/j.aoas.2013.01.012

[21] Prabha PH, B DP, Ishwariya S, Jashwanthi P, M SD. Valorization of Watermelon Rind as Dietary Chips Fortified with Composite Flour. 2021;9(8):591–6.

[22] Segmehl JS, Laromaine A, Keplinger T, May-Masnou A, Burgert I, Roig A. Magnetic wood by: In situ synthesis of iron oxide nanoparticles via a microwave-assisted route. J Mater Chem C. 2018;6(13):3395–402.

[23] Sharma JK, Srivastava P, Singh G, Akhtar MS, Ameen S. Biosynthesized NiO nanoparticles: Potential catalyst for ammonium perchlorate and composite solid propellants. Ceram Int [Internet]. 2015;41(1):1573–8. Available from: http://dx.doi.org/10.1016/j.ceramint.2014.09.093

[24] Iqbal J, Abbasi BA, Mahmood T, Hameed S, Munir A, Kanwal S. Green synthesis and characterizations of Nickel oxide nanoparticles using leaf extract of Rhamnus virgata and their potential biological applications. Appl Organomet Chem. 2019;33(8):0–2.

[25] Ezhilarasi AA, Vijaya JJ, Kaviyarasu K, Maaza M, Ayeshamariam A, Kennedy LJ. Green synthesis of NiO nanoparticles using Moringa oleifera extract and their biomedical applications: Cytotoxicity effect of nanoparticles against HT-29 cancer cells. J Photochem Photobiol B Biol [Internet]. 2016;164:352–60. Available from: http://dx.doi.org/10.1016/j.jphotobiol.2016.10.003

[26] Kundu M, Karunakaran G, Kuznetsov D. Green synthesis of NiO nanostructured materials using Hydrangea paniculata flower extracts and their efficient application as supercapacitor electrodes. Powder Technol [Internet]. 2017;311(3):132–6. Available from: http://dx.doi.org/10.1016/j.powtec.2017.01.085

[27] Helan V, Prince JJ, Al-Dhabi NA, Arasu MV, Ayeshamariam A, Madhumitha G, et al. Neem leaves mediated preparation of NiO nanoparticles and its magnetization, coercivity and antibacterial analysis. Results Phys [Internet]. 2016;6:712–8. Available from: http://dx.doi.org/10.1016/j.rinp.2016.10.005

[28] Angel Ezhilarasi A, Judith Vijaya J, Kaviyarasu K, John Kennedy L, Ramalingam RJ, Al-Lohedan HA. Green synthesis of NiO nanoparticles using Aegle marmelos leaf extract for the evaluation of in-vitro cytotoxicity, antibacterial and photocatalytic properties. J Photochem Photobiol B Biol [Internet]. 2018;180:39–50. Available from: https://doi.org/10.1016/j.jphotobiol.2018.01.023

[29] Abbasi BA, Iqbal J, Mahmood T, Ahmad R, Kanwal S, Afridi S. Plant-mediated synthesis of nickel oxide nanoparticles (NiO) via Geranium wallichianum: Characterization and different biological applications. Mater Res Express. 2019;6(8).

[30] Boonyanitipong P, Kositsup B, Kumar P, Baruah S, Dutta J. Toxicity of ZnO and TiO2 Nanoparticles on Germinating Rice Seed Oryza sativa L. Int J Biosci Biochem Bioinforma. 2011;1(4):282–5.

[31] Cañas JE, Long M, Nations S, Vadan R, Dai L, Luo M, et al. Effects of functionalized and nonfunctionalized single-walled carbon nanotubes on root elongation of select crop species. Environ Toxicol Chem. 2008;27(9):1922–31.

[32] Lin D, Xing B. Root uptake and phytotoxicity of ZnO nanoparticles. Environ Sci Technol. 2008;42(15):5580–5.

[33] Stampoulis D, Sinha SK, White JC. Assay-dependent phytotoxicity of nanoparticles to plants. Environ Sci Technol. 2009;43(24):9473–9.

[34] Palombari R. Influence of surface acceptor-donor couples on conductivity and other electrochemical properties of nonstoichiometric NiO at 200 °C. J Electroanal Chem. 2003;546(SUPP):23–8.

[35] Nowsath M, Theivasanthi T, Alagar M. Nickel Oxide Nanoparticles Thermal. Nanosci Nanotechnol. 2012;2:134–8.

[36] Prasad C, Gangadhara S, Venkateswarlu P. Bio-inspired green synthesis of Fe3O4 magnetic nanoparticles using watermelon rinds and their catalytic activity. Appl Nanosci. 2016;6(6):797–802.

[37] Holzwarth U, Gibson N. The Scherrer equation versus the 'Debye-Scherrer equation' Nat Publ Gr [Internet]. 2011;6(9):534. Available from: http://www.nature.com/doifinder/10.1038/nnano.2011.145%5Cnpapers2://publication/doi/10.1038/nnano.2011.145

[38] Teoh LG, Li KD. Synthesis and characterization of NiO nanoparticles by solgel method. Mater Trans. 2012;53(12):2135–40.

[39] Srihasam S, Thyagarajan K, Korivi M, Lebaka VR, Mallem SPR. Phytogenic generation of NiO nanoparticles using stevia leaf extract and evaluation of their in-vitro antioxidant and antimicrobial properties. Biomolecules. 2020;10(1).

[40] Li X, Zhang X, Li Z, Qian Y. Synthesis and characteristics of NiO nanoparticles by thermal decomposition of nickel dimethylglyoximate rods. Solid State Commun. 2006;137(11):581–4.

[41] Tauc J. OPTICAL PROPERTIES AND ELECTRONIC STRUCTURE OF AMORPHOUS Ge AND Si. Mat Res Bul. 1968;3:37–36.

[42] Varkey AJ, Fort AF. Solution growth technique for deposition of nickel oxide thin films. Thin Solid Films. 1993;235(1–2):47–50.

[43] Jeyaseelan SC, Premkumar R, Kaviyarasu K, Franklin Benial AM. Spectroscopic, quantum chemical, molecular docking and in vitro anticancer activity studies on 5-Methoxyindole-3-carboxaldehyde. J Mol Struct [Internet]. 2019;1197:134–46. Available from: https://doi.org/10.1016/j.molstruc.2019.07.042

[44] Kumari L, Li WZ, Vannoy CH, Leblanc RM, Wang DZ. Vertically aligned and interconnected nickel oxide nanowalls fabricated by hydrothermal route. Cryst Res Technol. 2009;44(5):495–9.

[45] Khodakovskaya M V., De Silva K, Biris AS, Dervishi E, Villagarcia H. Carbon nanotubes induce growth enhancement of tobacco cells. ACS Nano. 2012;6(3):2128–35.

[46] Singh A, Hussain I, Singh NB, Singh H. Uptake, translocation and impact of green synthesized nanoceria on growth and antioxidant enzymes activity of Solanum lycopersicum L. Ecotoxicol Environ Saf [Internet]. 2019;182(October 2018):109410. Available from: https://doi.org/10.1016/j.ecoenv.2019.109410

[47] Singh A, Singh NB, Hussain I, Singh H, Yadav V, Singh SC. Green synthesis of nano zinc oxide and evaluation of its impact on germination and metabolic activity of Solanum lycopersicum. J Biotechnol [Internet]. 2016;233:84–94. Available from: http://dx.doi.org/10.1016/j.jbiotec.2016.07.010